ResearchGate

See discussions, stats, and author profiles for this publication at: https://www.researchgate.net/publication/228603684

Comparison of Axial Dispersion and Tanks-in-Series Models for Simulating the Performance of Enzyme Reactors

ARTICLE *in* INDUSTRIAL & ENGINEERING CHEMISTRY RESEARCH · OCTOBER 2003

Impact Factor: 2.59 · DOI: 10.1021/ie030131j

CITATIONS
8

READS
199

2 AUTHORS, INCLUDING:

Ibrahim Abu Reesh
Qatar University
36 PUBLICATIONS **341** CITATIONS

SEE PROFILE

Available from: Ibrahim Abu Reesh
Retrieved on: 01 February 2016

Comparison of Axial Dispersion and Tanks-in-Series Models for Simulating the Performance of Enzyme Reactors

Ibrahim M. Abu-Reesh* and Basel F. Abu-Sharkh

Chemical Engineering Department, King Fahd University of Petroleum & Minerals, Dhahran 31261, Saudi Arabia

A comparison of two modeling approaches for simulating the performance of enzyme reactors using the axial dispersion and tanks-in-series models is described. The two modeling approaches are compared for the steady-state performance of enzyme reactors assuming Michaelis−Menten kinetics with competitive product inhibition. The performance of the reactors is described in terms of substrate conversion and yield. The equation $Pe = 2(N - 1)$ is used to correlate the parameter of the dispersion model (*Pe*) with that of the tanks-in-series model (*N*) for the entire range of dispersion from plug flow to CSTR. The predictions of the two models agree well, especially at low dimensionless residence times and high Peclet numbers. Practically, the predictions of the two models are essentially equivalent when the above equation is used to relate their two parameters. However, the tanks-in-series model is simpler and has computational advantages over the dispersion model, although its physical basis is not as clear as that of the dispersion model. Lactose hydrolysis by the enzyme β-galactosidase, which exhibits Michaelis−Menten kinetics with competitive product inhibition, is used as a model system in this study. The kinetic parameters for lactose hydrolysis are obtained from the literature.

Introduction

The continuous stirred tank reactor (CSTR) and plug-flow reactor (PFR) are two different ideal reactor models that are used for the description of flow reactors. The CSTR assumes perfect mixing, whereas the PFR assumes no mixing. No real reactor has precisely the characteristics of either of the two ideal reactors. The axial dispersion model (ADM) and tanks-in-series model (TISM) are one-parameter models that describe partially mixed reactors with a finite level of mixing, which cannot be described by either of the two ideal reactor models. The ADM is characterized by the Peclet number (*Pe*), which represents all of the effects that cause deviations from ideal PFR behavior, such as nonuniform velocity profiles or eddies. The *Pe* number is the single parameter in this model. As *Pe* increases from 0 to ∞, the flow pattern in the reactor changes from complete mixing (CSTR) to no mixing (PFR). The ADM requires solution of a second-order differential equation to compute the steady-state conversion. In addition, this model gives different results for different boundary conditions. In the TISM, the nonideal reactor is considered as being made up of a cascade of *N* equal-sized CSTRs arranged in series. *N* is the single parameter in this model. As *N* increases from 1 to ∞, the flow pattern in the reactor changes from complete mixing (CSTR) to no mixing (PFR). Although the physical basis of the TISM is not as clear as that of the ADM, the TISM is simple and can be used with any kinetic equation. The steady-state mathematical model of the TISM requires the solution of algebraic equations instead of a differential equation. The main defect of the TISM is that *N* takes only integer values. This limitation can be removed by using either the gamma function model[1] or the fractional tank model.[2] When *N* is allowed to take noninteger values, then the computational advantage is lost. Although the ADM and TISM are rather similar in many ways, there is no one exact way to compare them. However, the two models can be compared quantitatively by equating their variances. This leads to a relationship between their two parameters, *Pe* and *N*.

In the literature, there appears to be a lack of agreement in utilizing the TISM and ADM in the modeling of reactor systems including enzyme reactors, which have growing industrial applications. Kobayashi and Moo-Young (1971)[3] were the first to apply the dispersion model to immobilized enzyme reactors. Some authors[4] have pointed out that the ADM provides a satisfactory description only of mixing that does not deviate significantly from plug-flow behavior. Others[5] have emphasized that the application of the ADM for *Pe* values of less than 10 is not advised and, in this range, the TISM is more adequate. Turner and Mills (1990)[6] reported that the TISM is more realistic and advantageous compared to the ADM for simulating the performance of Fischer−Tropsch slurry bubble column reactors. Lee et al.[7] recommended a two-CSTRs-in-series model to represent activated sludge processes for treating municipal wastewater. Nardi et al.[8] showed that the single-parameter models (ADM and TISM) satisfactorily represent the flow pattern in horizontal flow anaerobic immobilized sludge reactors. Poughon et al.[9] described the hydrodynamics of a nitrifying fixed-bed column using a model including *N* tanks in series with back-mixing. Komolprasert and Ofoli[10] showed that the ADM is suitable for predicting the extent of starch liquefaction by *B. licheniformis* α-amylase during reactive extrusion. Using first-order enzyme kinetics, Komolprasert and Ofoli[10] reported that the ADM is suitable for analysis of enzymatic reactions up to 30% conversion.

* To whom correspondence should be addressed. Current address: Dr. Ibrahim M. Abu-Reesh, Chemical Engineering Department, The University of Jordan, Amman 11942, Jordan. E-mail: abureesh@ju.edu.jo.

10.1021/ie030131j CCC: $25.00 © 2003 American Chemical Society
Published on Web 10/03/2003

Using the equation $Pe = 2(N - 1)$ to relate the parameters of the two models, Elgeti[11] found good agreement between a pipe flow reactor and a series of ideally mixed reactors for first-order, second-order, and first-order successive reactions. Elgeti[11] showed that the equation $Pe = 2(N - 1)$ has a good theoretical basis. Others[12,13] also have used the same equation. Van Hasselt et al.[14] showed that, for the three levels of a porosity reactor, both the gas and liquid residence time distributions can be predicted with the TISM. Comparisons of the ADM and TISM by matching the variances led to a relationship between Pe and N. For small deviations from the PFR, the Pe number was found to be equal to $2N$, whereas for the whole range of dispersion, the equation $Pe = 2(N - 1)$ was used. Ponzi and Gonzalez[15] compared the ADM and TISM for a first-order reversible reaction using the same conversion and the same start-up time. Good agreement was found, especially at low Damkohler numbers and high Peclet numbers. In a recent paper, Dommeti and Balakotaiah[16] showed that there is an upper bound on the Damkohler number at which the predictions of the ADM and TISM begin to diverge. They derived an equation for this upper bound of the Damkohler number for different kinetic models. The objective of this work is to compare the predictions of the ADM and TISM for the performance of enzyme reactors. Reactor conversion and yield are determined for enzyme reactions described by Michaelis−Menten kinetics with competitive product inhibition. This study discusses the conditions under which the two models agree for predicting the performance of enzyme reactors. The equation $Pe = 2(N - 1)$ is used to relate the parameters of the two models. Milk (or whey) lactose conversion to glucose and galactose by the enzyme β-galactosidase is investigated using the two modeling approaches.

Model Development

Axial Dispersion Model. Consider an enzyme reactor of length L and fluid velocity u. Assuming axial dispersion, the steady-state material balance of the substrate (with concentration S) in the liquid is given by[17]

$$D_z \frac{d^2S}{dZ^2} - u\frac{dS}{dZ} - [-R(S,P)] = 0 \tag{1}$$

where D_z is the dispersion coefficient and Z is the longitudinal direction of flow. The boundary conditions of Danckwerts[18] at steady state require continuity of the flux at both ends of the reactor

$$\text{at } Z = 0 \qquad S = S_o + \frac{D_z}{u}\frac{dS}{dZ} \tag{2}$$

$$\text{at } Z = L \qquad \frac{dS}{dZ} = 0 \tag{3}$$

Assume that the enzymatic reaction follows Michaelis−Menten kinetics with competitive product inhibition and no enzyme deactivation; that is, assume that the reaction rate is given by

$$-R(S,P) = -\frac{dS}{dt} = \frac{V_{max}S}{K_m\left(1 + \frac{P}{K_i}\right) + S} \tag{4}$$

where V_{max} is the maximum reaction rate (mol/L·h), K_m is the Michaelis−Menten constant (mol/L), K_i is the inhibition constant (mol/L), and P is the product concentration (mol/L).

Further assume that no product is present in the reactor feed (i.e., $P_o = 0$). From reaction stoichiometry, one obtains

$$S_o = P + S \tag{5}$$

Using dimensionless variables, the above equations can be reduced to

$$\frac{1}{Pe}\frac{d^2\alpha}{dx} - \frac{d\alpha}{dx} - \theta\frac{\alpha}{K'_m + \alpha(1 - \zeta) + \zeta} = 0 \tag{6}$$

$$\text{at } x = 0 \qquad \alpha = 1 + \frac{1}{Pe}\frac{d\alpha}{dx} \tag{7}$$

$$\text{at } x = 1 \qquad \frac{d\alpha}{dx} = 0 \tag{8}$$

where

$$x = \frac{Z}{L}, \quad \alpha = \frac{S}{S_o}, \quad K'_m = \frac{K_m}{S_o}, \quad \zeta = \frac{K_m}{K_i}, \quad Pe = \frac{uL}{D_z}, \quad \theta = \frac{V_{max}\tau}{S_o}$$

The dimensionless Peclet number (Pe) characterizes the mixing characteristics in the reactor. When Pe approaches ∞, negligible dispersion is observed (plug-flow reactor). When Pe approaches 0, large dispersion is observed (mixed reactor).

Judging from eqs 6−8, it is clear that the performance of the reactor depends on θ, Pe, ζ, and K'_m.

Tanks-in-Series Model. Consider a series of N CSTRs of equal size. Substrate balance over the ith stage at steady state gives

$$\tau_i = \frac{S_{i-1} - S_i}{-R(S_i,P_i)} = \frac{S_{i-1} - S_i}{\frac{V_{max}S_i}{K_m\left(1 + \frac{P_i}{K_i}\right) + S_i}} \qquad i = 1, 2, ..., N \tag{9}$$

Using dimensionless parameters, the dimensionless residence time θ for reactor i is given by

$$\theta_i = \frac{(\alpha_{i-1} - \alpha_i)}{\alpha_i}[K'_m + \zeta(1 - \alpha_i) + \alpha_i] \qquad i = 1, 2, ..., N \tag{10}$$

where

$$\alpha = \frac{S}{S_o} \quad \text{and} \quad \theta = \frac{V_{max}\tau}{S_o}$$

Solving eq 10 for α_i gives

$$\alpha_i = \frac{1}{2a}[-b \mp \sqrt{b^2 - 4ac}] \qquad i = 1, 2, ..., N \tag{11}$$

where

$$a = (1 - \zeta), \quad b = \theta_i + K'_m + \zeta, \quad c = -(K'_m + \zeta)\alpha_{i-1}$$

That is, for each reactor i, the value of α can be determined from α of the previous reactor $i-1$.

In the tanks-in-series model, the number of reactors N describes the mixing characteristics of the reactor, where $N = 1$ represents perfect mixing and $N = \infty$ represents plug-flow conditions.

Solutions of the Models

Axial Dispersion Model. Solution of this model requires numerical integration of a nonlinear second-order differential equation to obtain the reactor conversion. The reverse shooting method[19] and the double precision IMSL library[20] subroutine DBVPMS were used to solve eq 6 with the boundary conditions given by eqs 7 and 8. The dimensionless substrate concentration at the reactor exit, α_L, can be obtained at a given dimensionless residence time θ if the parameters K'_m, Pe, and ζ are known.

For the special case in which the Michaelis−Menten constant (K_m) and the inhibition constant K_i are equal (i.e., $\zeta = 1$), the rate of the enzymatic reaction reduces to first-order kinetics

$$\frac{1}{Pe}\frac{d^2\alpha}{dx^2} - \frac{d\alpha}{dx} - \frac{\theta\alpha}{K'_m + 1} = 0 \tag{12}$$

$$\text{at } x = 0 \qquad \alpha = 1 + \frac{1}{Pe}\frac{d\alpha}{dx} \tag{13}$$

$$\text{at } x = 1 \qquad \frac{d\alpha}{dx} = 0 \tag{14}$$

The analytical solution for eqs 12−14 is given by

$$\alpha_L = \frac{4q\exp(Pe/2)}{(1+q)^2\exp(qPe/2) - (1-q)^2\exp(-qPe/2)} \tag{15}$$

where

$$q = \sqrt{1 + \frac{4\theta}{Pe(1+K'_m)}}$$

This solution was first obtained by Danckwerts in 1953.[18]

When $Pe \to \infty$, the design equation for the plug-flow reactor can be obtained.

$$\theta_{PFR} = (1-\zeta)(1-\alpha_L) - (K'_m + \zeta)\ln\alpha_L \tag{16}$$

For $\zeta = 1$

$$\theta_{PFR} = (K'_m + 1)\ln\frac{1}{\alpha_L} \tag{17}$$

Tanks-in-Series Model. The effluent dimensionless substrate concentration (α_N) of reactor N can be obtained by applying eq 11 sequentially. That is, the outlet of reactor $i-1$ becomes inlet for reactor i, and this is repeated for $i = 1-N$. In this work, a Fortran computer program was used to calculate the dimensionless substrate concentration. The total dimensionless residence time can then be calculated by adding the residence times for all N equal-sized reactors in series. For the special case of $\zeta = 1$, eq 10 reduces to

$$\theta_i = (K'_m + 1)\left(\frac{\alpha_{i-1}}{\alpha_i} - 1\right) \qquad i = 1, 2, ..., N \tag{18}$$

Solving for α_i gives

$$\alpha_i = \frac{\alpha_{i-1}}{\left(\frac{\theta_i}{K'_m + 1}\right) + 1} \qquad i = 1, 2, ..., N \tag{19}$$

Applying eq 19 for $i = 1$ to $i = N$, an expression for α_N can be obtained as

$$\alpha_N = \frac{1}{\left[\left(\frac{\theta_i}{K'_m + 1}\right) + 1\right]^N} = \frac{1}{\left[\frac{\theta_{N,total}}{N(K'_m + 1)}\right]^N} \tag{20}$$

where

$$\theta_{N,total} = \sum_{i=1}^{N}\theta_i \qquad i = 1, 2, ..., N \tag{21}$$

From eqs 20 and 21, the total dimensionless residence time can be related to the dimensionless exit substrate concentration of the last reactor $i = N$ by

$$\theta_{N,total} = N(K'_m + 1)(\alpha_N^{-1/N} - 1) \tag{22}$$

Reactor Performance

Two criteria for reactor performance are used in this study.

1. Substrate Conversion (X). In the dispersion model, the conversion is given by

$$X = 1 - \alpha_L \tag{23}$$

In the tanks-in-series model, the conversion is given by

$$X = 1 - \alpha_N \tag{24}$$

For the $\zeta = 1$ case

$$X = 1 - \frac{1}{\left[\frac{\theta_{N,total}}{N(K'_m + 1)}\right]^N} \tag{25}$$

For the PFR with $\zeta = 1$

$$X = 1 - \alpha_{PFR} = 1 - \exp\left(-\frac{\theta_{PFR}}{K'_m + 1}\right) \tag{26}$$

2. Yield (Y). The yield is defined here as the ratio of the amount of substrate converted to the maximum amount that could be converted during one residence time.[21,22]

In the dispersion model, the yield is given by

$$Y = \frac{S_o - S_L}{V_{max}\frac{L}{u}} = \frac{1-\alpha_L}{\theta} = \frac{X}{\theta} \tag{27}$$

In the tanks-in-series model, the yield is given by

$$Y = \frac{S_o - S_N}{V_{max}\tau_{N,total}} = \frac{1-\alpha_N}{\theta_{N,total}} = \frac{X}{\theta_{N,total}} \tag{28}$$

Relations between Pe and N

A comparison between the ADM and TISM can be made by equating the variances of the two models.

Table 1. Conditions for Case Studies 1 and 2

parameter	case study 1	case study 2
reactor temperature (°C)	40	7
K_m (mol/L)	0.023 27[a]	5.206×10^{-4}[a]
K_i (mol/L)	0.015 34[b]	5.206×10^{-4}[b]
S_o (wt %)	5	5
$K'_m = K_m/S_o$	0.159	3.561×10^{-3}
$\zeta = K_m/K_i$	1.517	1

[a] From eq 32. [b] From eq 33.

Using the closed boundary conditions of Danckwerts,[18] the following relation can be obtained

$$N = \frac{Pe^2}{2(Pe - 1 + e^{-Pe})} \tag{29}$$

For small deviations from plug flow (very large Pe), eq 29 reduces to

$$Pe = 2N \tag{30}$$

Equation 31 below is also used to relate Pe and N.[11−13,23] By expanding the dispersion model equation in a Taylor series, Elgeti[11] derived this relation between Pe and N. This equation describes the whole range of dispersion between complete mixing and no mixing, including the two limits.

$$Pe = 2(N - 1) \quad \text{or} \quad N = Pe/2 + 1 \tag{31}$$

When $Pe = 0$, $N = 1$ (one CSTR), and when $Pe = \infty$, $N = \infty$ (PFR).

Case Studies

The enzymatic conversion of lactose to glucose and galactose by the enzyme β-galactosidase is examined as a model system. This reaction is described by Michaelis−Menten kinetics with competitive product (galactose) inhibition.[24] Milk and whey lactose hydrolysis is important for nutritional, physiological, technological, and environmental reasons. The kinetic constants for the enzymatic lactose hydrolysis are taken from the literature as shown in eqs 32 and 33.[24,25]

$$K_m = \exp\left(28.54 - \frac{10\,110}{T}\right) \quad \text{(mol/L)} \tag{32}$$

$$K_i = \exp\left(24.58 - \frac{9001}{T}\right) \quad \text{(mol/L)} \tag{33}$$

The enzyme is quite stable for temperatures up to 40 °C.[24] Typical lactose content of milk or whey (S_o) is about 5 wt % (0.1462 mol/L). Two case studies were conducted. The conditions for the two case studies are listed in Table 1. Under the conditions of case study 2, the kinetic equation reduces to first-order kinetics.

Dimensionless Residence Time at Which the ADM and TISM Begin To Diverge. To determine the range of θ at which the predictions of the two models begin to diverge for the case of $\zeta = 1$,where an analytical solution is available for the ADM, the ratio of the exit substrate concentration for the TISM and ADM is obtained by dividing eq 20 by eq 15 and using eq 29 to relate Pe and N.[16]

$$\frac{S_N}{S_L} = \frac{(1+q)^2 \exp\left(Pe\frac{q}{2}\right) - (1-q)^2 \exp\left(-Pe\frac{q}{2}\right)}{4q \exp(Pe/2)\left[1 + \theta\left(\frac{2}{Pe} - \frac{2}{Pe^2}(1 - e^{-Pe})\right)\right]^{1/[2/Pe - (2/Pe^2)(1-e^{-Pe})]}} = g(\theta, Pe) \tag{34}$$

For the case of $Pe \gg 1$, for which eq 30 is applicable, the asymptotic form of the function g can be determined to be[16]

$$g(\theta, Pe) \approx \exp\left[\frac{Pe}{2}\left(\frac{1}{6}\theta_i^3 - \frac{3}{8}\theta_i^4 + \cdots\right)\right] \tag{35}$$

where θ_i, the dimensionless residence time for reactor i, is given by

$$\theta_i = \frac{\theta}{N} = \frac{2\theta}{Pe}$$

For $\theta_i \ll 1$, retaining only the first term in the asymptotic expansion, one obtains

$$\frac{S_N}{S_L} \approx \exp\left(\frac{\theta^3}{6N^2}\right) \tag{36}$$

Defining the exponent in eq 36 as β, this means that the exit concentrations predicted by the two models differ by a factor of β, where

$$\beta = \frac{\theta^3}{6N^2} = \frac{2\theta^3}{3Pe^2} \quad \text{or} \quad \theta = 1.15\beta^{1/3}Pe^{2/3} \tag{37}$$

Dommeti and Balakotaiah[16] used $\beta = 1$ to define the point of divergence of the two models. They defined θ^* as the value of θ at which the two exit concentrations differ by at most a factor of e. Thus, θ^* is given by

$$\theta^* = 1.15Pe^{2/3} \qquad (\text{for } Pe \gg 1) \tag{38}$$

Dommeti and Balakotaiah[16] used θ^* to differentiate between slow and fast reactions, with $\theta < \theta^*$ for slow reactions and $\theta > \theta^*$ for fast reactions.

For first-order kinetics and dispersion close to perfect mixing (i.e., $Pe \to 0$, $N \to 1$), Dommeti and Balakotaiah[16] derived the following relation between θ^* and Pe

$$\theta^* = \frac{7.21}{Pe} \quad (\text{for } Pe \to 0) \tag{39}$$

From eq 39, it is clear that, as $Pe \to 0$, the value of θ^* at which the two models begin to diverge becomes very large. Equations 38 and 39 are valid for first-order enzyme kinetics ($\zeta = 1$), as $K'_m \ll 1$. For large K'_m values, the dimensionless residence time θ has to be divided by $K'_m + 1$, as given in eq 12.

Results and Discussions

Figure 1 shows the conversions predicted by both the ADM ($Pe \approx 0$) and one-CSTR ($N = 1$) model as a function of the dimensionless residence time, θ; the dimensionless Michaelis−Menten constant, K'_m; and the ratio of the Michaelis−Menten constant to inhibition constant, ζ. The Pe value used in Figure 1 is 0.0001 to avoid division by zero in the ADM. Equation 31 [i.e., Pe

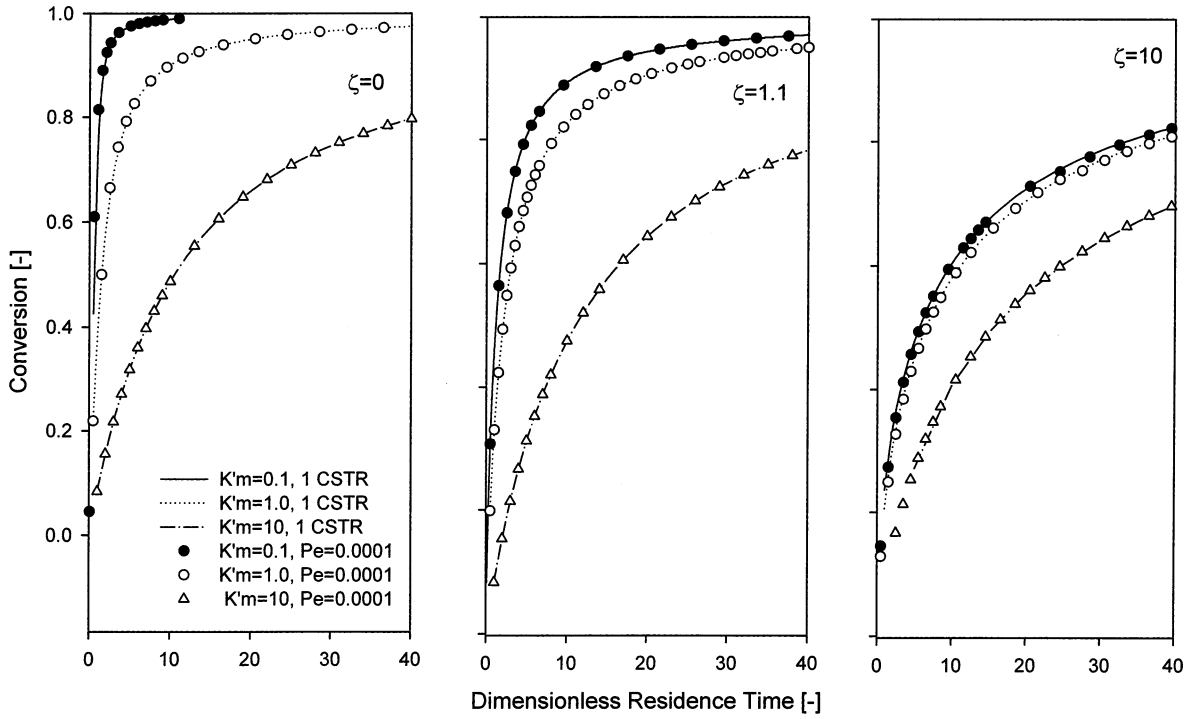

Figure 1. Conversion vs dimensionless residence time for $N = 1$ and $Pe = 0.0001$

$= 2(N - 1)]$ is used to relate Pe and N. It is clear that this equation represents the complete-mixing limit correctly (i.e., $Pe = 0$ and $N = 1$). Three values of ζ are used in Figure 1 (0, 0.1, and 10). $\zeta = 0$ corresponds to Michaelis−Menten kinetics with no inhibition by the product. Increasing the value of ζ increases the product inhibition. Three values of K'_m are also shown in the figure (0.1, 1, and 10). From Figure 1, it is clear that increasing θ increases the substrate conversion and increasing K'_m reduces the conversion because the rate of reaction decreases with increasing K'_m. At very low values of K'_m ($K'_m \rightarrow 0$), the enzyme kinetics approaches zeroth-order, whereas at very high values of K'_m ($K'_m \rightarrow \infty$), the enzyme kinetics approaches first-order. Also from Figure 1, it can be seen that increasing the value of ζ reduces the conversion. This is expected because the product inhibition reduces the rate of the enzymatic reaction. It is clear from Figure 1 that both the ADM and the TISM agree very well in predicting the enzyme reactor conversion using eq 31 to relate the parameters of the two models, Pe and N. Actually, the two models are identical when $Pe \rightarrow 0$ and $N \rightarrow 1$. Equation 31 represents the perfect-mixing limit of the dispersion range correctly and is simpler than eq 29. Equation 30 predicts $Pe \rightarrow 2$ instead of $Pe \rightarrow 0$ at complete mixing.

Figure 2a shows the substrate conversion predicted from the ADM at $Pe = 2$ and the TISM at $N = 2$ according to eq 31 describing the relationship between Pe and N. A conversion trend similar to that of Figure 1 is obtained. Comparing Figure 1 and Figure 2a shows that increasing Pe increases the conversion. This is expected for such an enzyme kinetic equation. Comparing the values of conversion predicted by the two models in Figure 2a shows that they agree well, especially at low dimensionless residence times, θ (low Damkholer numbers or slow reactions). Deviations occur only at high dimensionless residence times (high conversions).

Using eq 29 to relate the parameters of the two models (Pe and N), larger deviations were observed in the predicted conversions of the two models than were obtained using eq 31. Figure 2b shows the conversion predicted by the TISM at $N = 2$ and the ADM at $Pe = 2.557$ (according to eq 29). The deviation in conversion is larger, especially at high dimensionless residence times, although the simpler relation $Pe = 2(N - 1)$ gives smaller errors than the variance-matching procedure for large dimensionless residence times. There is no explanation or justification for this observation. In Figure 2a and b, it is clear that the ADM predicts higher conversions than the TISM at high dimensionless residence times.

Decreasing the intensity of mixing with increasing values of N and Pe improved the agreement between the two models. Figure 3 shows the conversions predicted using the TISM with $N = 3$ and the ADM with $Pe = 4$, according to eq 31. Similar results were obtained for the case of $N = 5$ and $Pe = 8$, as shown in Figure 4. As will be shown later, in the low-dispersion region (high Pe), the higher the Pe, the higher the θ at which the two models begin to diverge.

Figure 5 shows the predicted yields from both the TISM with $N = 5$ and the ADM with $Pe = 8$ as a function of the dimensionless residence time, θ; the dimensionless Michaelis−Menten constant, K'_m; and the ratio of the Michaelis−Menten constant to the inhibition constant, ζ. It is clear from Figure 5 that the yield decreases with increasing dimensionless residence time, i.e., high yields are predicted for slow reactions and visa versa. As given by eqs 27 and 28, the yield is equal to the conversion divided by the dimensionless residence time. The effect of K'_m on the yield is more important in the case of slow reactions with no product inhibition, as increasing the K'_m value decreases the yield. At high ratio of the Michaelis−Menten constant to the inhibition constant ($\zeta = 10$), the K'_m value has little effect on the reactor yield, especially at high dimensionless residence times (fast reactions). It is also clear from Figure 5 that the yield decreases with increasing ζ, especially for low values of K'_m. Again, in Figure 5, an excellent agreement is observed between

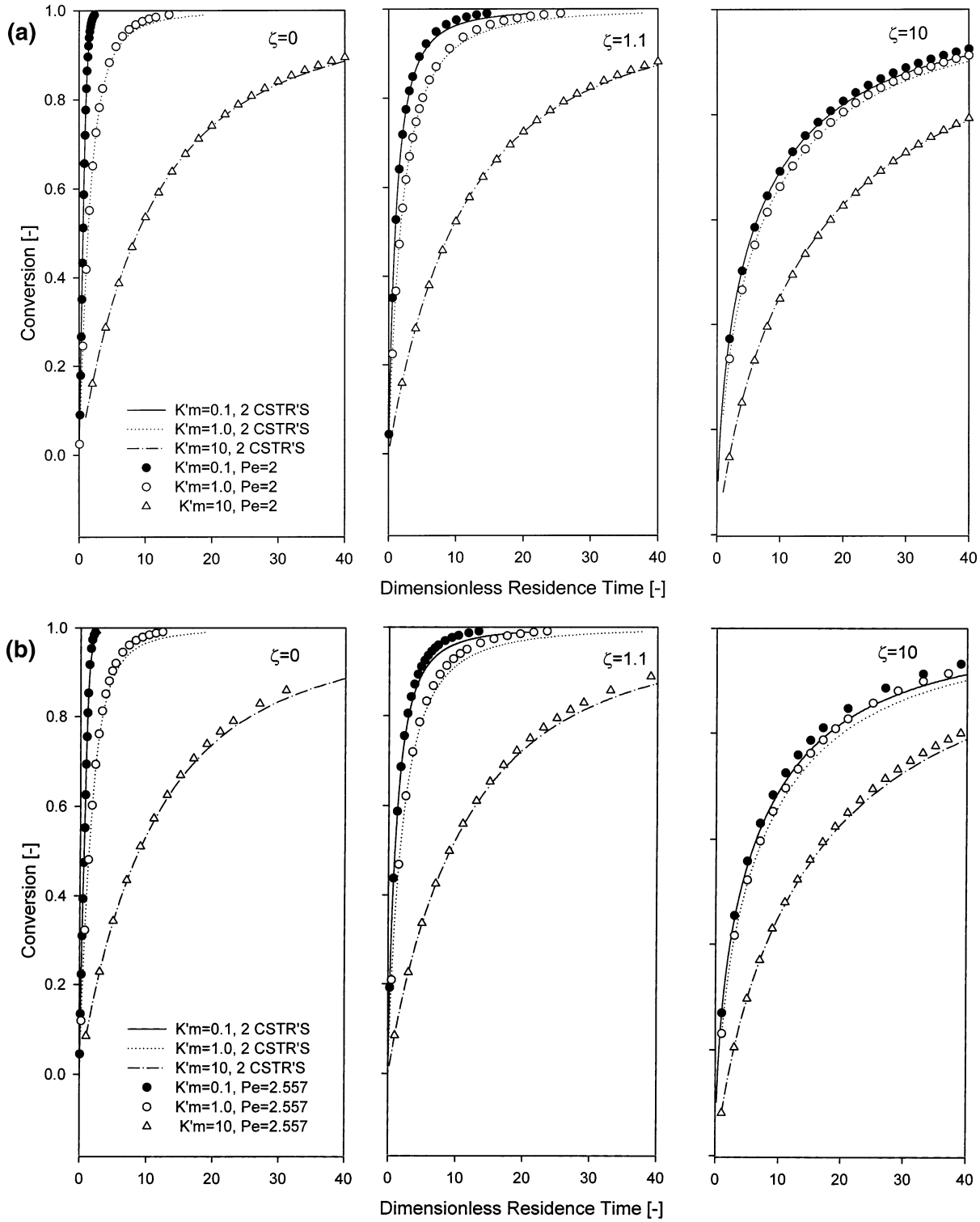

Figure 2. Conversion vs dimensionless residence time for $N = 2$ and (a) $Pe = 2$ and (b) $Pe = 2.557$.

the yields predicted by the TISM ($N = 5$) and the ADM ($Pe = 8$). This is expected because a high level of agreement is obtained in the predicted conversions, as shown in Figure 4, and the yield depends on the conversion and the dimensionless residence time, as given by eqs 27 and 28.

The conversion of milk (or whey) lactose to glucose and galactose by the enzyme β-galactosidase was studied using the two modeling approaches as discussed above in the case studies. Figure 6 describes the first case study ($K'_m = 0.159$ and $\zeta = 1.517$), which corresponds to lactose hydrolysis at a reactor temperature of 40 °C. The x coordinate in Figure 6 is $1/Pe$ for the ADM and $1/[2(N - 1)]$ for the TISM. The x coordinates of the two models are equal if we use eq 31 to relate the parameters of the two models. In Figure 6, the symbols represent points for $N = 2-11$ CSTRs in series, whereas the continuous lines represent the results for the ADM. From Figure 6, it is clear that conversion increases with increasing dimensionless residence time and decreases with increasing intensity of mixing. The effect of the intensity of mixing is important only at high values of the dimensionless residence time (fast reactions). As shown in Figure 6, the conversions predicted

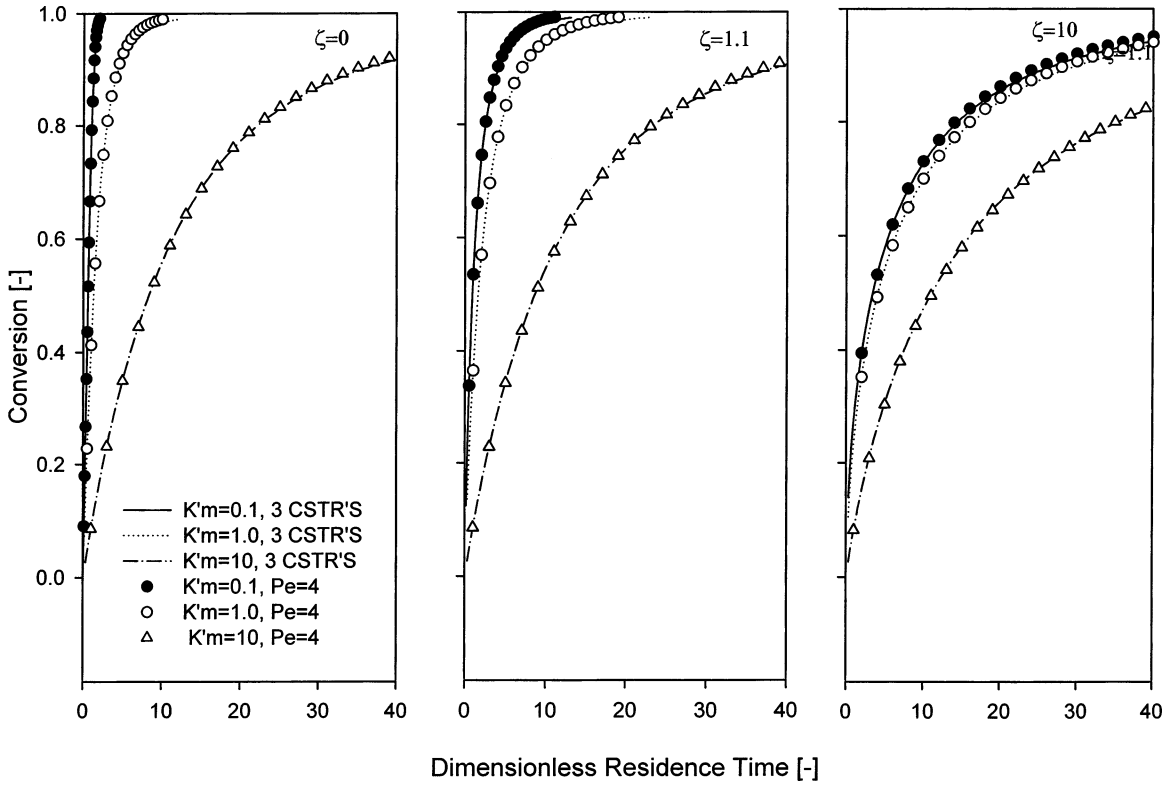

Figure 3. Conversion vs dimensionless residence time for $N = 3$ and $Pe = 4$.

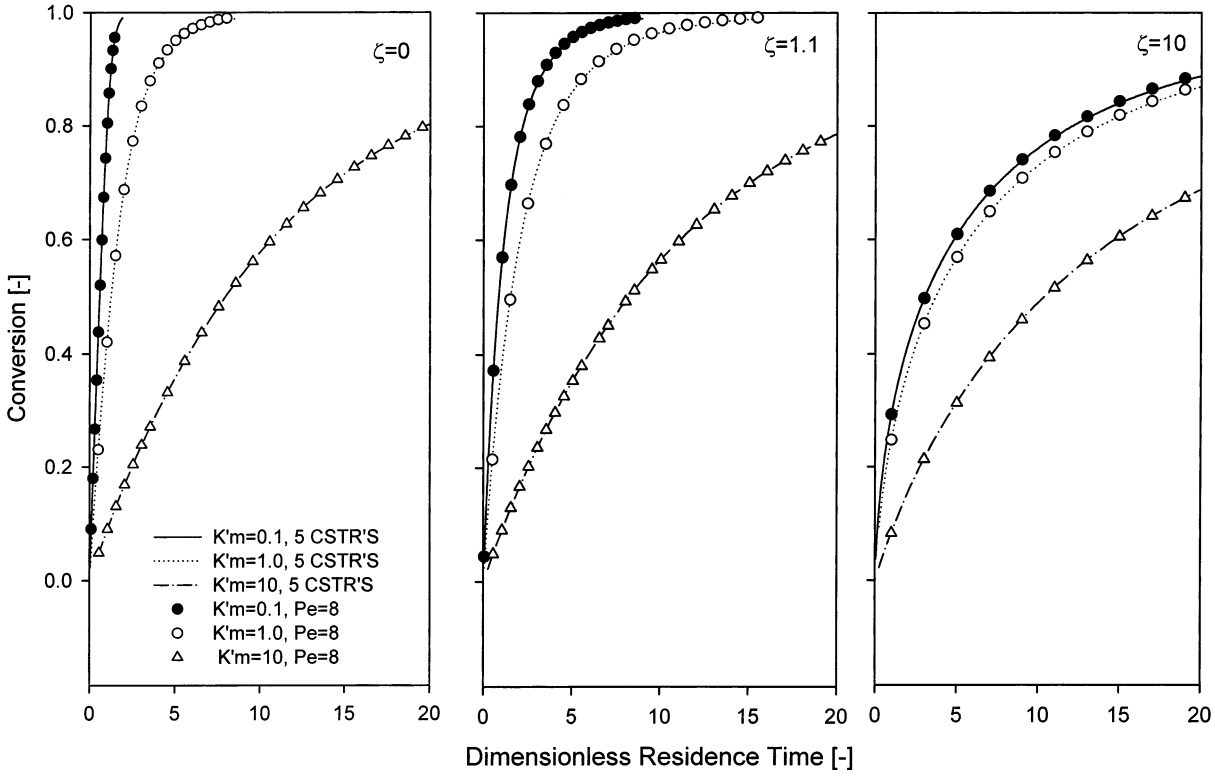

Figure 4. Conversion vs dimensionless residence time for $N = 5$ and $Pe = 8$.

by the two models agree well, and deviations can be observed only at high θ and high intensity of mixing such as $N = 2$.

For first-order reactions, both the ADM and the TISM are easy to apply. When $\zeta = 1$, the axial dispersion model for Michaelis−Menten kinetics with competitive product inhibition reduces to first-order kinetics with the analytical solution given by eq 15. The second case study ($\zeta = 1$, $K_m = K_i = 5.206 \times 10^{-4}$ mol/L) corresponds to lactose hydrolysis at 7 °C.[24] Figure 7 shows the conversions predicted by the ADM and TISM as a function of dimensionless residence time for $\zeta = 1$. The N values shown in the figure are 1, 2, 3, and 5, and the corresponding Pe numbers are 0, 2, 4, and 8, respectively, according to eq 31. The PFR conversion is also shown in Figure 7 for comparison. The difference in the

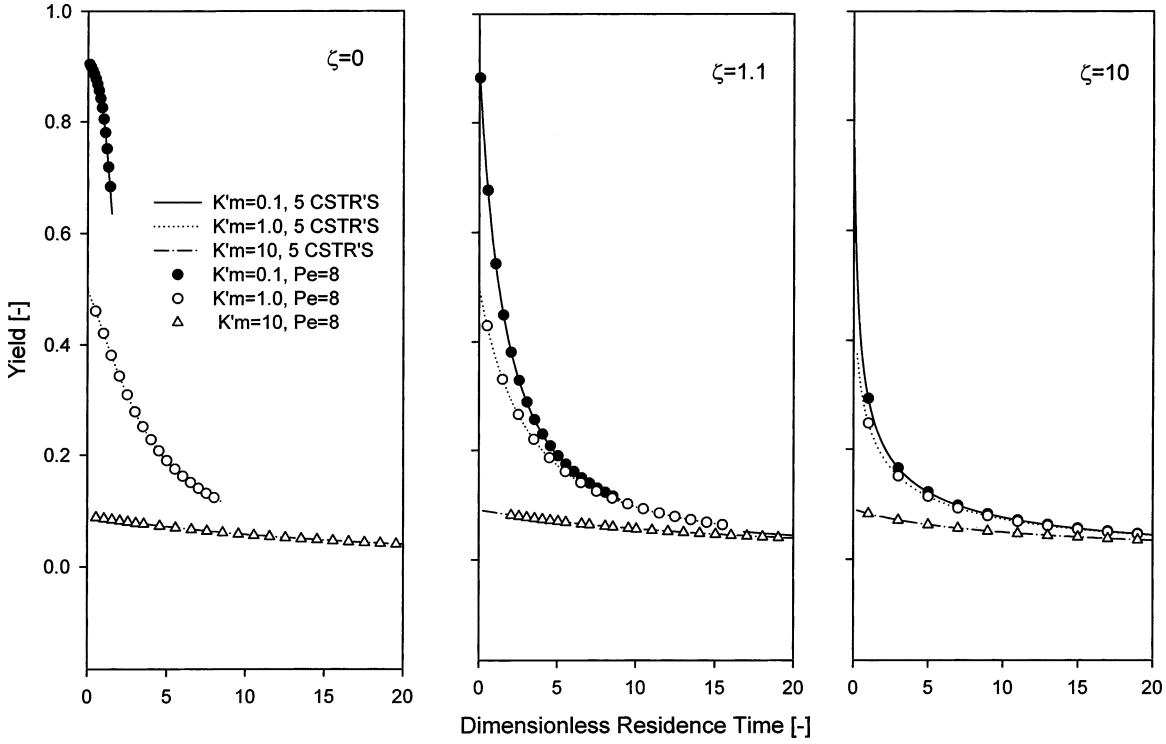

Figure 5. Yield vs dimensionless residence time for $N = 5$ and $Pe = 8$.

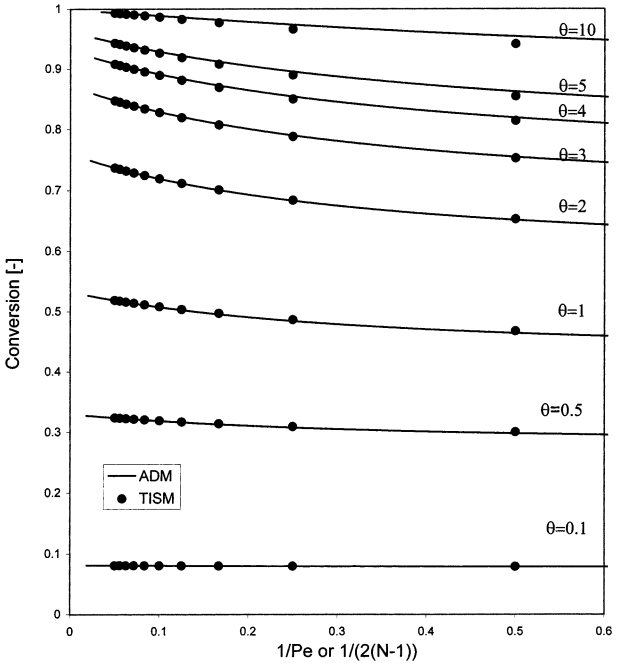

Figure 6. Lactose conversion using dispersion and tanks-in-series models at 40 °C ($K'_m = 0.159$ and $\zeta = 1.517$).

conversions predicted by the two models is very small. For $N = 1$ and $Pe = 0$, the two models are equivalent. The largest absolute difference in the conversions predicted by the two models is 0.0125 for $N = 2$ and $Pe = 2$. This difference decreases with increasing N and Pe. For $N = 3$ and $N = 5$, the largest absolute differences in the predicted conversions between the two models are 0.007 47 and 0.003 39, respectively.

For the case of $\zeta = 1$, K'_m is very small (3.561×10^{-3} mol/L). For $K'_m \ll 1$, eqs 38 and 39 are applied to our kinetic equation. θ^* is the dimensionless residence time at which the exit concentrations of the two models differ by at most a factor of e. To determine the range of θ at which the predictions of the two models diverge, the ratio of the exit substrate concentrations for the TISM and ADM is plotted as a function of θ in Figure 8a for $Pe = 100$ and $Pe = 50$. The corresponding values of θ^* (according to eq 38) are 24.8 and 15.6, respectively. At low θ ($\theta < \theta^*$, slow reactions), the predictions of the two models agree very well. At high θ ($\theta > \theta^*$, fast reactions), the predictions of the two models diverge. In practice, most conversion is achieved at $\theta < \theta^*$. For example, most commercial processes operate at lactose conversion level of 80% or greater.[26] Figure 8b shows the same comparisons between the two models but for $Pe < 10$. For first-order kinetics ($\zeta = 1$) and ADM close to perfect mixing, i.e., $Pe \rightarrow 0$ ($N \rightarrow 1$), Dommeti and Balakotaiah[16] derived eq 39 which relates θ^* and Pe in this mixing region. From eq 39, it is clear that, as $Pe \rightarrow 0$, the value of θ^* at which the two models begin to diverge becomes very large. For example, in Figure 8b, when $Pe = 0.0001$, $\theta^* = 72\,100$ (from eq 39). This is very close to the case of $Pe = 0$ for the ADM and $N = 1$ for the TISM, where the two models are equivalent. It can be seen from Figure 8a and b that the ADM and TISM agree very well at low θ and high Pe. Divergence occurs only at very high θ (high conversion) especially for low Pe. As shown in Figure 8a and b, the ADM always predicts higher conversions than the TISM at very high dimensionless residence times. In the case of small dimensionless residence times θ (low Da),the difference $S_N - S_L$ is third-order in θ for the variance-matching method (eq 29),[16] whereas this difference is quadratic in θ using the equation $Pe = 2(N - 1)$. It should be clear that it makes no sense to compare the exit concentrations of the two models at very large θ ($Da \rightarrow \infty$).

The predictions of the two models can be compared for $\zeta \neq 1$ by using a numerical solution for the ADM boundary value problem as shown above. For nonlinear kinetics, such as Michaelis−Menten with competitive product inhibition, the upper limit of θ_u for which the

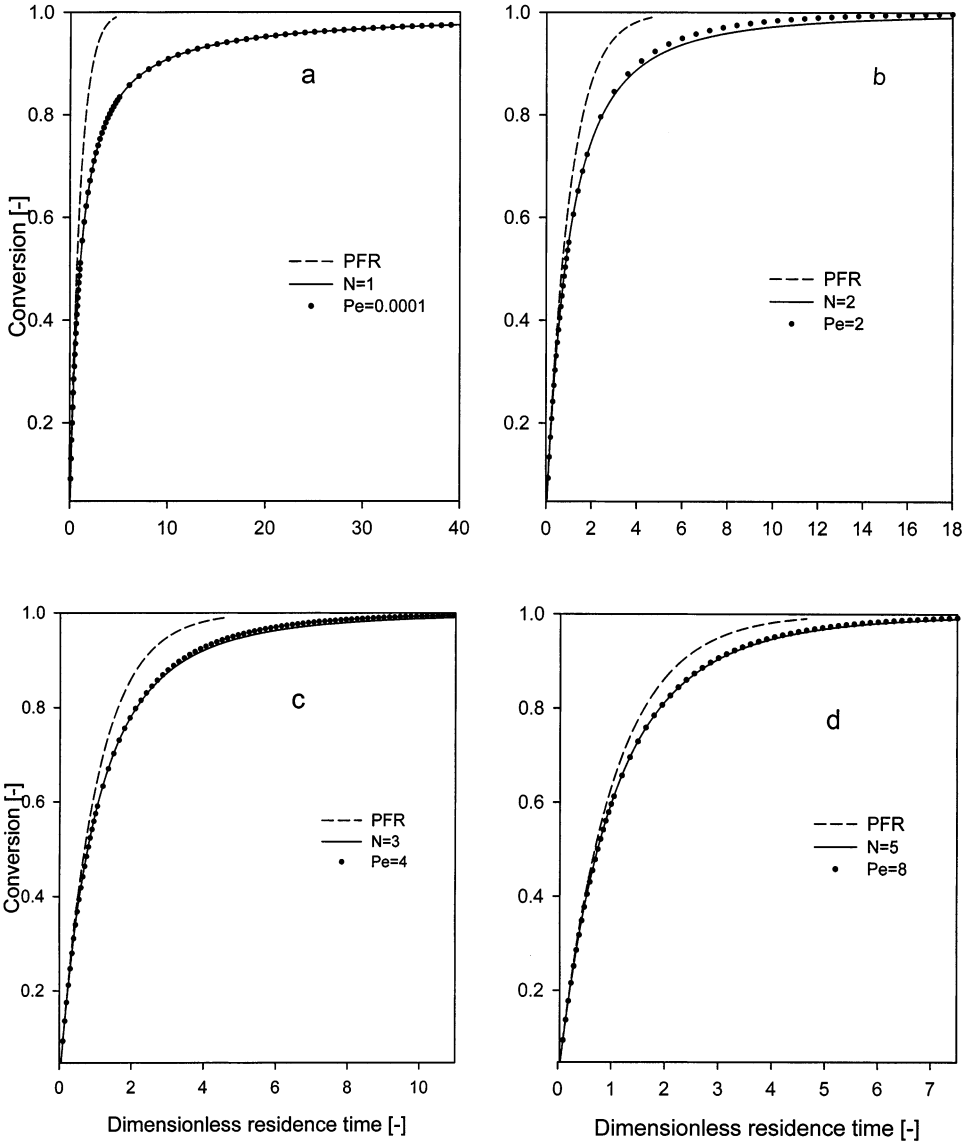

Figure 7. Lactose conversion vs dimensionless residence time for $\zeta = 1$ (temperature = 7 °C) and initial lactose concentration = 5 wt %.

predictions of the two models agree is given by[16]

$$\theta_u = \frac{1.15Pe^{2/3}}{|f'(S_N)|} \quad \text{for } Pe \to \infty\ (N \to \infty) \qquad (40)$$

$$\theta_u = \frac{7.21}{Pe|f'(S_N)|} \quad \text{for } Pe \to 0\ (N \to 1) \qquad (41)$$

where $|f'(S_N)|$ is the absolute value of the first derivative with respect to concentration of the normalized reaction rate at the exit concentration. For $\theta < \theta^*$ (slow reactions), the predictions of the two models agree well. For $\theta > \theta^*$ (fast reactions), the predictions of the two models diverge , and the TISM cannot be used to describe the ADM.

Conclusions

Two modeling approaches based on the ADM and TISM were developed for simulating the steady-state performance of a reactor performing enzymatic reactions described by Michaelis−Menten kinetics with competitive product inhibition.

The equation $Pe = 2(N - 1)$ was found to describe the relationship between Pe and N for the whole range of dispersion between plug flow and complete mixing, including the two limits $Pe \to 0$ ($N \to 1$) and $Pe \to \infty$ ($N \to \infty$). Using this equation, the conversions and yields predicted by the two models were found to agree well, especially at high Peclet numbers and low dimensionless residence times.

Differences between the predictions of the two models appear only at very high dimensionless residence times. Simulation results showed that there is an upper bound on the dimensionless residence time, θ^*, at which the predictions by the two models begin to diverge. This upper bound on θ depends on Pe. In the low-dispersion region, the higher Pe, the higher θ^*. For the case of infinite dispersion ($Pe \to 0$, $N \to 1$), the θ^* value at which the two models begin to diverge is very large. For $Pe = 0$ and $N = 1$, the two models are identical. In general, using the simple equation $Pe = 2(N - 1)$, the difference between the conversions predicted by the two models disappears for practical purposes. However, the tanks-in-series model presents computational advantages compared to dispersion model.

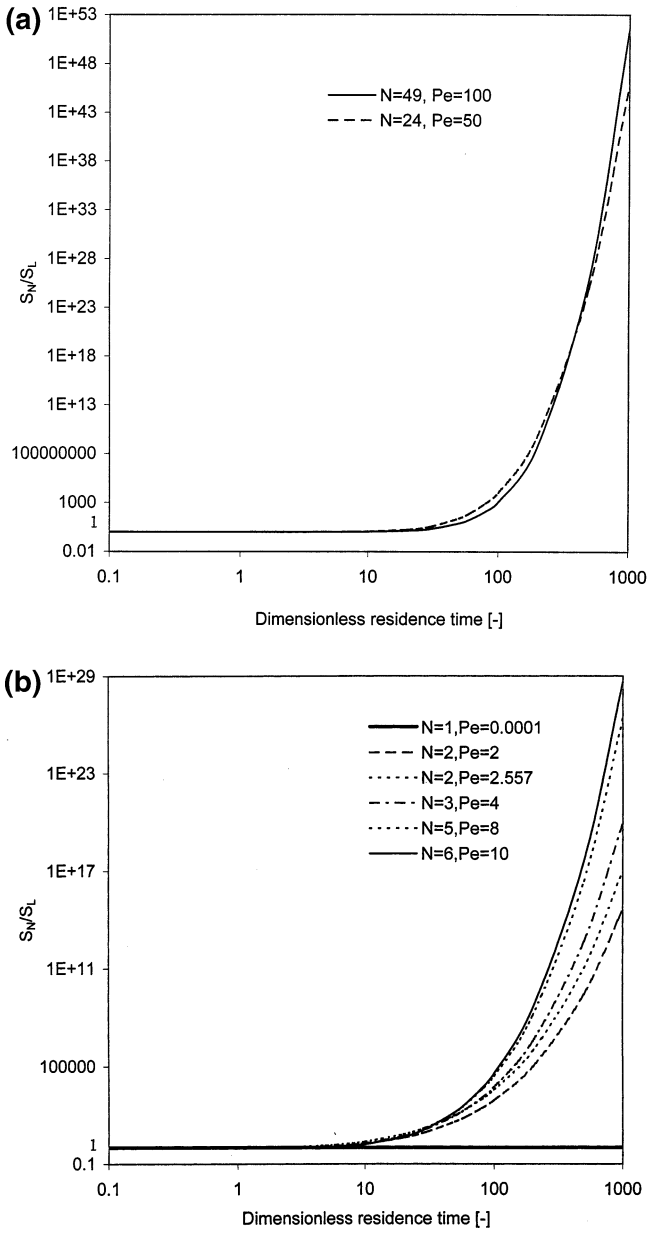

Figure 8. Ratio of exit concentrations for the TISM and ADM as a function of dimensionless residence time, $\zeta = 1$, for (a) $Pe = 50$, 100 and (b) $Pe \leq 10$.

For equal Michaelis−Menten and inhibition constants ($\zeta = 1$), the nonlinear Michaelis−Menten kinetics with competitive product inhibition is reduced to first-order kinetics, allowing the dispersion equation with Danckwerts boundary conditions to be solved analytically. The enzymatic conversion of lactose to glucose and galactose is examined as a model system. Lactose conversion is determined at the two temperatures of 40 and 7 °C. Lactose hydrolysis is described by first-order kinetics at 7 °C ($\zeta = 1$), which allows the ADM to be solved analytically.

Acknowledgment

The authors acknowledge the support provided by King Fahd University of Petroleum & Minerals,-Dhahran, Saudi Arabia.

Nomenclature

a, b, c = parameters defined in eq 11
D_z = axial dispersion coefficient (m^2/h)
$f(\alpha)$ = normalized reaction rate [$f(1) = 1$]
$g(\theta,Pe)$ = function defined in eq 34
K_i = inhibition constant (mol/L)
K_m = Michaelis−Menten constant (mol/L)
K'_m = dimensionless Michaelis−Menten constant (K_m/S_o)
L = reactor length (m)
N = number of mixed tanks in series
P = product concentration (mol/L)
q = parameter defined in eq 15
$R(S,P)$ = reaction rate (mol/L·h)
S = substrate concentration (mol/L)
t = time (h)
T = temperature (K)
u = interstitial liquid velocity (m/h)
V_{max} = maximum reaction rate (mol/L·h)
X = substrate conversion
x = dimensionless axial distance (Z/L)
Y = yield
Z = axial distance in the reactor (m)

Greek Letters

α = dimensionless substrate concentration (S/S_o)
β = deviation parameter (defined in eq 37)
ζ = dimensionless ratio of (K_m/K_i)
τ = residence time (h)
θ = dimensionless residence time ($V_{max}\tau/S_o$)

Dimensionless Numbers

Da = Damkohler number ($V_{max}\tau/S_o$)
Pe = Peclet number (uL/D_z)

Subscripts and Superscripts

i = refers to the ith reactor
L = effluent
N = refers to the Nth reactor
o = initial
PFR = plug-flow reactor
total = total of all reactors
Z = axial direction
* = critical value for linear kinetics
u = upper bound

Abbreviations

ADM = axial dispersion model
CSTR = continuous stirred tank reactor
PFR = plug-flow reactor
TISM = tanks-in-series model

Literature Cited

(1) Buffham, B. A.; Gibilaro, L. G. A generalization of the tanks in series mixing model. *AIChE J*. **1968**, *14*, 805−806.

(2) Stokes, R. L.; Nauman, E. B. Residence time distribution functions for stirred tanks in series. *Can. J. Chem. Eng.* **1970**, *48*, 723−725.

(3) Kobayashi, T.; Moo-Young, M. Backmixing and mass transfer in the design of immobilized enzyme reactors. *Biotechnol. Bioeng.* **1971**, *13*, 893−910.

(4) Wen, C. Y.; Fan, L. T. *Models for Flow Systems and Chemical Reactors*; Marcel Dekker: New York, 1975.

(5) Shinnar, R. Use of residence and contact time distributions in reactor design. In *Chemical Reaction and Reactor Engineering*; Carberry, J., Varma, A., Eds.; Marcel Dekker: New York, 1987.

(6) Turner, J. R.; Mills, P. L. Comparison of axial dispersion and mixing cell models for design and simulation of Fischer−Tropsch slurry bubble column reactors. *Chem. Eng. Sci.* **1990**, *45* (8), 2317−2324.

(7) Lee, T. T.; Wang, F. Y.; Newell, R. B. A generalized procedure for modeling and simulation of activated sludge plant using lumped-parameter approach. *J. Environ. Sci. Health A* **1997**, *32* (1), 83−104.

(8) Nardi, I. R.; Zaiat, M.; Foresti, E. Influence of the tracer characteristics on hydrodynamic models of packed bed reactors. *Bioprocess Eng.* **1999**, *21* (5), 469−476.

(9) Poughon, L.; Dussap, C. G.; Gros, J. B. Dynamic model of a nitrifying fixed bed column: Simulation of the biomass distribution of *Nitrosomonas* and *Nitrobacter* and of transient behavior of the column. *Bioprocess Eng.* **1998**, *20* (3), 209−221.

(10) Komolprasert, V.; Ofoli, R. Y. A dispersion model for predicting the extent of starch liquefaction by *B. licheniformis* α-amylase during reactive extrusion. *Biotechnol. Bioeng.* **1991**, *37*, 681−690.

(11) Elgeti, K. A new equation for correlating a pipe flow reactor with a cascade of mixed reactors. *Chem. Eng. Sci.* **1996**, *51*, 5077−5080.

(12) Kramers, H.; Alberda, G. Frequency response analysis of continuous flow systems. *Chem. Eng. Sci.* **1953**, *2*, 173−181.

(13) Aris, R. End and beginnings in the mathematical modeling of chemical engineering systems. *Chem. Eng. Sci.* **1993**, *48* (14), 2507−2517.

(14) Van Hasselt, B. W.; Calis, H. P. A.; Sie, S. T.; Van den Bleek, C. M. Gas- and liquid-phase residence time distribution in the three levels of porosity reactor. *Chem. Eng. Sci.* **1999**, *54*, 5047−5053.

(15) Ponzi, E. N.; Gonzalez, M. G. Comparison between the dispersion and tanks in series models. *Chem. Eng. Sci.* **1980**, *35* (8), 1804−1806.

(16) Dommeti, S. M. S.; Balakotaiah, V. On the limits of validity of effective dispersion models for bulk reactions. *Chem. Eng. Sci.* **2000**, *55*, 6169−6186.

(17) Fogler, H. S. *Elements of Chemical Reaction Engineering*, 3rd ed.; Prentice Hall: Upper Saddle River, NJ, 1999.

(18) Danckwerts, P. V. Continuous flow systems, Distribution of residence times. *Chem. Eng. Sci.* **1953**, *2* (1), 1−18.

(19) Nauman, E. B. *Chemical Reactor Design*; John Wiley and Sons: New York, 1987.

(20) IMSL Software, Visual Numerics, Inc.: Houston, TX, 1987 (support@imsl.com).

(21) Lortie, R. Evaluation of the performance of immobilized enzyme reactors with Michaelis−Menten kinetics. *J. Chem. Technol. Biotechnol.* **1994**, *60*, 189−193.

(22) Abu-Reesh, I. M. Predicting the performance of immobilized enzyme reactors using reversible Michaelis−Menten kinetics. *Bioprocess Eng.* **1997**, *17* (3) 131−137.

(23) Balakotaiah, V. Some comments on "A new equation for correlation of a pipe flow reactor with a cascade of mixed reactors". *Chem. Eng. Sci.* **1998**, *53* (9), 1787.

(24) Santos, A.; Ladero, M.; Garcia-Ochoa, F. Kinetic modeling of lactose hydrolysis by β-galactosidase from *Kluyveromices fragillis*. *Enzyme Microb. Technol.* **1998**, *22*, 558−567.

(25) Abu-Reesh, I. M. Optimal design for CSTRs in series performing enzymatic lactose hydrolysis. *Bioprocess Eng.* **2000**, *23* (6), 709−713.

(26) Yang, S. T.; Okos, M. R. Effects of temperature on lactose hydrolysis by immobilized β-galactosidase in plug-flow reactor. *Biotechnol. Bioeng.* **1989**, *33*, 873−885.

Received for review February 12, 2003
Revised manuscript received July 25, 2003
Accepted August 19, 2003

IE030131J